Black carbon (BC) in North Tibetan Mountain; Effect of Kuwait fires on glacier

Jiamao Zhou[1,6], Xuexi Tie[1,2], Baiqing Xu[3], Shuyu Zhao[1], Mo Wang[3], Guohui Li[1], Ting Zhang[1], Zhuzi Zhao[1,7],Suixin Liu[1], Song Yang[3], Luyu Chang[4,5], Junji Cao[1]

[1]KLACP, SKLLQG, Institute of Earth Environment, Chinese Academy of Sciences, Xi'an 710061, China

[2]Center for Excellence in Urban Atmospheric Environment, Institute of Urban Environment, Chinese Academy of Sciences, Xiamen 361021, China

[3]Key Laboratory of Tibetan Environment Changes and Land Surface Processes, Institute ofTibetan Plateau Research, Chinese Academy of Sciences, Beijing 100101, China

[4]Shanghai Meteorological Service, Shanghai, 200030, China

[5]Shanghai Key Laboratory of Meteorology and Health, Shanghai, 200030, China

[6] University of Chinese Academy of Sciences, Beijing 100049, China

[7] School of Chemistry & Environmental Engineering, Jiangsu University of Technology

Correspondence to: Xue Xi Tie (tiexx@ieecas.cn) or Baiqing Xu (baiqing@itpcas.ac.cn)

Abstract. The BC deposition on the ice core at Muztagh Ata Mountain, Northern Tibetan Plateau was analyzed. Two sets of measurements were used in this study, which included the air samplings of BC particles during 2004-2006 and the ice core drillings of BC deposition during 1986-1994. Two numerical models were used to analyze the measured data. A global chemical transportation model (MOZART-4) was used to analyze the BC transport from the source regions, and a radiative transfer model (SNICAR) was used to study the effect of BC on snow albedo. The results show that during 1991-1992, there was a strong spike of the BC deposition at Muztagh Ata, suggesting that there was an unusual emission in the upward region during this period. This high peak of BC deposition was investigated by using the global chemical transportation model (MOZART-4). The analysis indicated that the emissions from large Kuwait fires at the end of the first Gulf War in 1991 caused this high peak of the BC concentrations and deposition (about 3-4 times higher than other years) at the Muztagh Ata Mountain, suggesting that the upward BC emissions had important impacts on this remote site located in Northern Tibetan Plateau. Thus, there is a need to quantitatively estimate the effect of surrounding emissions on the BC concentrations in the northern Tibetan Plateau. In this study, a sensitive study with 4 individual BC emission regions (Central Asia, Europe, Persian Gulf, and South Asia) was conducted by using the MOZART-4 model. The result suggests that during the "normal period" (non Kuwait Fires), the largest effect was due to the Central Asia source (44%) during Indian monsoon period, while during non-monsoon period, the largest effect was due to the South Asia source (34%). The increase of radiative forcing increase (RFI) due to the deposition of BC on snow was estimated by using the radiative transfer model (SNICAR). The results shows that under the fresh snow assumption, the estimated increase of RFI ranged from 0.2 W m^{-2} to 2.5 W m^{-2}, while under the aged snow assumption, the estimated increase of RFI ranged from 0.9 W m^{-2} to 5.7 W m^{-2}. During the Kuwait fires period, the RFI values increased about 2-5 times higher than the "normal period", suggesting a significant increase for the snow melting in Northern Tibetan Plateau due to this fire event. This result suggests that the variability of BC deposition at the Muztagh Ata Mountain provides useful information to study the effect of the upward BC emissions on environmental and climate issues in the Northern Tibetan Plateau. The radiative effect of BC deposition on the snow melting provides important information regarding the water resources in the region.

Key Words; Northern Tibetan glaciers, BC deposition, MOZART model

1 Introduction

Black carbon (BC) particles emitted from combustion are considered as an important air pollutant, as they have direct effect by absorbing and scattering solar radiation, and indirect effect by the change of cloud microphysical process (acting as ice nuclei) and efficiency of precipitation (acting as cloud condensation nuclei) (Ramanathan et al., 2001). Albedo changes induced by strongly light absorbing component by deposited on the surface of snow and ice are key parameters to govern the radiative forcing and accelerate melting (Holben et al., 1998; Hansen and Nazarenko, 2004). These important properties make BC as a key topic related with climate change but are not well understood due to the very different inhomogeneous spatial and temporal distribution of BC, especially in remote areas, such as the Tibetan Plateau.

BC particles can deposit and preserve in the ice by the progress of post-deposition on the glaciers and ice sheets. Retrieved ice cores from remote mountain glaciers and ice sheets provide useful information of the historical BC aerosol emissions and synchronous meteorology conditions. Previous studies on records of carbonaceous aerosols show that the emissions of fossil fuel combustion from Central Europe had significant impact on the glacier in the Swiss Alps (Lavanchy et al., 1999). Bisiaux et al., (2012) analyzed two ice cores dirlled in Antarctica and found that the ice core records of BC deposition reflected the change of atmospheric BC emission, distribution and transport in Southern Hemisphere. By using an ice core in Greenland, the BC emissions from industrial activities and forest fires are differentiated (McConnell et al. 2007). These researches indicate that BC records in history are important and practicable method to investigate the regional aerosol transport and emission variations.

In this study, the ice core BC at Muztagh Ata, Northern Tibetan Plateau is analyzed. Identification the source regions, which have important impact on BC deposition at Muztagh Ata is very important scientific issue, because of its location. In particularly, there was a strong spike of the BC deposition during 1992-1993 at Muztagh Ata (as shown in the following text), reflecting that there was unusual emission in the upward region from Muztagh Ata. This strong spike of the ice core BC was about 3-4 times higher than other years, producing important effects on climate and hydrological cycle.

As a result, the study of the sources of BC, which affect the ice core BC in this location, needs to be carefully studied. Muztagh Ata locates in the east of Pamir and the north of Tibetan Plateau. The ice core data provides important information for atmospheric circulation and climate change in Asia (An et al., 2001). Moreover, the climate in Muztagh Ata is very sensitive to solar warming mechanisms because it has a large snow cover in the region, resulting in important impacts on the hydrological cycle of the continent by enhancing glacier melt.

The BC sources which contribute the BC deposition in Tibetan Plateau have been previously studied. Their results show that BC deposited on glaciers of the Pamir Mountains was emmited from Europe, Middle East and central Asia (Liu et al., 2008; Xu et al., 2009a; Wang et al., 2015b), whereas BC deposition on snow and ice over the Himalayas and southeastern Tibetan Plateau was mainly affected by the western upward regions in winter. During the Indian summer monsoon season, they were mainly affected by the BC sources in Indian region (Ming et al., 2008; Xu et al., 2009b; Kaspari et al., 2011; Wang et al., 2015a). However, at present, the effects of the transport pathways and individual contributions of BC sources to the Muztagh Ata region have not been carefully studied. Because the radiative forcing caused by BC in snow and ice between different regions is very different, depending upon the emitting intensities, ocean-land distributions, topography, regional atmospheric circulations, and other factors, detailed study on the source contributions to the region as well as the climate effect are needed to carefully study this important region.

Both the ice core deposition measurements at Muztagh Ata and a global chemical model (MOZART-4; Model for Ozone and Related chemical Tracers, version 4) are used in this study. To better evaluate the model performance, the air samples of BC particles during 2004-2006 were also analyzed. The global chemical transport model (MOZART-4) was used to analyze the long-term trend in the early 90s of the observed BC deposition and to quantify the individual contribution of different BC sources to the deposition on the snow cover. The modeled temporal variations and magnitude of the BC concentrations in the atmosphere and snow were compared to observations. Finally, a radiative transfer model (SNICAR) was used to study the effect of BC on snow albedo, radiative forcing, and runoff changes induced by the BC deposition on the Muztagh Ata snow.

2 Methodologies

2.1 Sampling Sites

Muztagh Ata Mountain is located in the north side of Tibetan Plateau. Both atmospheric sampling and ice core drilling BC were conducted at the Muztagh Ata site. The atmospheric sampling BC (38°17.30'N, 75°01.38'E) was conducted in the Cold and Arid Regions Environmental and Engineering Institute, Chinese Academy of Sciences, at a 4500 m above sea level (a.s.l.). A 170.4 m ice core (9.5 cm in diameter) was drilled during the summer season in 2012 from Kuokuosele (KKSL) Glacier of Muztagh Ata (38°11'N, 75°11'E, 5700 m a.s.l.), which was conducted by the Institute of Tibetan Plateau Research, Chinese Academy of Sciences. Because the site is surrounded by several important BC source regions, this measurement site is suitable to investigate the effect of BC emissions on north part Tibetan Plateau, which plays important roles for global climate and hydrology (see Fig. 1).

The average annual temperature at the peak of the mountain is approximately -20^{o}C. Because the numerous high mountains block the warm and humid air currents from Indian and Pacific Ocean, the climate in this area is relatively dry. The averaged annual precipitation is less than 200 mm, which is mainly snow to form perennial glaciers. There are 128 modern glaciers and on average about 377 square kilometers. The prevailing winds in this region are usually westerly jet stream. Previous studies suggested that there was very small effect by local sources, and the aerosol pollutions were originated mainly from the west by mid- and long-range transport. During summer, the South Asia monsoon had also important effect on the transport of BC particles from India (Liu et al., 2008; Wu et al., 2008; Zhao et al., 2011; Wang et al., 2015b).

2.2 Measurements

During the period from December 5, 2003 to February 17, 2006, Eighty-one valid total suspended aerosol particle (TSP) were obtained with custom-made samplers at flow rates of 16 l min^{-1}. The measurements were conducted under very difficult

environmental conditions, because of its high mountain location. The sampler power was supplied by solar energy and a storage battery. Each sample was collected over one week and on 15 mm Whatman quartz microfibre filter (QM/A, Whatman LTD, Maidstone, UK), which was pre-combusted at 800^{o}C for 3 hours to remove the potential carbon disturbance. The sample was identified as valid when its sampling standard volume was greater than 30 m^{3}. As a result, the valid sample numbers for spring, summer, autumn, and winter were 19, 21, 14, and 27, respectively.

For the ice core measurement, a 170.4 m ice core (9.5 cm in diameter) was drilled during the summer season in 2012 from Kuokuosele (KKSL) Glacier of Muztagh Ata (38°11'N, 75°11'E, 5700 m a.s.l.), which is close to the BC air sampling site. A stainless steel scalpel that pre-cleaned at -5^{o}C in a class 100 laminar flow bench was used to remove outer layer of the ice core to exclude the pollutants that might be mixed in during drilling, transport, and storage. The ice core dating and calculation of BC deposition fluxes were provided by Institute of Tibetan Plateau Research, Chinese Academy of Science. The detailed method for the measurement of BC deposition is shown by Xu et al. (2009a).

2.3 Analytical methods

The elemental carbon (EC, which is proxy to BC in this study) analyses for atmospheric filters (TSP samples) were carried out by using Desert Research Institute (DRI) Model 2001 carbon analyzer (Atmoslytic Inc., Calabasas, CA, USA) with IMPROVE (Interagency Monitoring of PROtected Visual Environments) thermal/optical reflectance (TOR) protocol (Chow et al., 1993; Chow et al., 2004). A 0.526 cm^{2} punch of a quartz filter sample was heated in a stepwise manner to obtain data for three elemental carbon (EC) fractions. At the same time, OP (pyrolyzed carbon) was produced at <580 ^{o}C in the inert atmosphere which decreases the reflected light to correct for charred OC. Total EC is the sum of the three EC fractions minus OP. More details and QAQC (Quality Assurance and Quality Control) are shown by Cao et al. (2003) and Cao et al., (2009).

The rBC (refractory black carbon), which is used instead of BC for measurements derived from incandescence methods (Petzold et al., 2013), was analyzed at Institute

of Tibetan Plateau Research, Chinese Academy of Sciences by using a Single Particle Soot Photometer (SP2) coupled with an ultrasonic nebulization system (CETAC UT5000). The mass of rBC of individual particles were measured by using a laser-induced incandescence (Schwarz et al., 2006). The incandescence signal can be converted to rBC mass which is detected by photomultiplier tube detectors. Previous studies has successfully applied this analytical method to ice cores researches (McConnell et al., 2007; Kaspari et al., 2011; Bisiaux et al., 2012). Detailed description on the SP2 analytical process and calibration procedures can be found in (Wendl et al., 2014) and (Wang et al., 2015b).

Although the differences in the two analytical techniques (Wang et al., 2015b), in order to facilitate the discussions, they are uniformly referred to as black carbon (BC) in our study since both of them are materials share some of the characteristics of BC with its light-absorbing properties (Petzold et al., 2013).

2.4 Global chemistry transport model / MOZART-4

The model used in this study is MOZART-4 (Model for Ozone and Related chemical Tracers, version 4). The model is an offline global chemical transport model for the troposphere developed jointly by the National Center for Atmospheric Research (NCAR), the Geophysical Fluid Dynamics Laboratory (GFDL), and the Max Planck Institute for Meteorology (MPI-Met). The detailed model description and model evaluated can be found in Emmons et al. (2010). The aerosol modules was developed by Tie et al. (2005). This model have been developed and used to quantify the global budget of trace gases and aerosol particles, and to study their atmospheric transport, chemical transformations and removal (Emmons et al., 2010; Chang et al., 2016). The model is built base on the framework of the Model of Atmospheric Transport and Chemistry (MATCH) (Rasch et al., 1997). Convective mass fluxes are diagnosed by using the shallow and mid-level convective transport formulation of Hack (Hack, 1994) and deep convection scheme (Zhang and McFarlane, 1995). Vertical diffusion within the boundary layer is built on the parameterization by Holtslag and Boville (1993). Advective transport scheme used the flux form semi-Lagrangian transport algorithm (Lin and Rood, 1996). The wet deposition includes in-cloud as well as below-cloud scavenging developed by Brasseur et al. (1998) is taken into

MOZART-4. Details of the chemical solver scheme can be found in the Auxiliary Material (Kinnison et al., 2007).

In the present study, the model includes 85 gas-phase species, 12 bulk aerosol compounds and approximately 200 reactions. The horizontal resolution of this study is 1.9°×2.5° with 56 hybrid sigma-pressure vertical levels from the surface to approximately 2 hPa. The meteorological initial and boundary conditions are down load from NCAR Community Data Portal (CDP), using National Centers for Environmental Prediction (NCEP) meteorology. The model transport of this study is driven by the Modern-Era Retrospective-analysis for Research and Applications (MERRA) 6-hour reanalysis data with a 1.9°×2.5° grid provided by National Aeronautics and Space Administration (NASA).

The BC emission inventory used in this global model is based on the simulation of the POET (Precursors of Ozone and their Effects in the Troposphere) database from 1997 to 2007 and the data of BC emission inventory including fossil fuel and biofuel combustion from a previous study (Bond et al., 2004; Bond et al., 2007). Figure 2 illustrates the updated 21-year average global BC emissions from 1986 to 2006. There are two types of black carbon particles in MOZART-4, hydrophobic and hydrophilic particles. Hydrophobic particles are directly emitted from the sources, and are converted to hydrophilic in the atmosphere (Hagen et al., 1992; Liousse et al., 1993; Parungo et al., 1994), with a rate constant of 7.1×10^{-6}/s (Cooke and Wilson, 1996).

2.5 BC deposition estimation

In order to compare to the measured ice core BC deposition at the Muztagh Ata Mountain, the BC deposition flux is calculated in this study. In the estimation, the calculated atmospheric BC concentrations and precipitation data obtained from China Meteorological Data Service Center were compiled and evaluated. In addition, annual BC deposition parameters and deposition flux calculation methods were described in other studies (Jurado et al., 2008; Yasunari et al., 2010; Fang et al., 2015; Li et al., 2017). In brief, deposition fluxes are calculated by the following equations:

$$F_{DD} = 10^{-4} v_D C_{BC}\, t \quad (1)$$

$$F_{WD} = 10^{-7} p_0 W_p C_{BC} \quad (2)$$

$$F_{BC} = F_{DD} + F_{WD} \quad (3)$$

where 10^{-4} and 10^{-7} are unit conversion factors; F_{DD} and F_{WD} are the annual dry and wet deposition (ng cm^{-2}), respectively; the total BC deposition flux (F_{BC}) (ng cm^{-2}) is the sum of $F_{DD}$and F_{WD}; where v_D (m s^{-1}) is the dry deoposition velocity of black carbon; t is total estimation time for one year (s); $p_0$is the annual precipitation rate (mm); W_p is the particle washout ratio (dimensionless); and C_{BC} is the annual atmospheric BC concentrations at Muztagh Ata Mountain (ng m^{-3}). There are large differences in estimates on v_D and W_p (Jurado et al., 2005; Jurado et al., 2008; Yasunari et al., 2013). A fixed small dry deposition velocity of 1.0×10^{-4} m s^{-1} onto snow was adopted (Yasunari et al., 2010; Nair et al., 2013) and the corresponding estimation values are likely to represent a lower bound for BC dry deposition in this area. Particle washout ratio W_p is assumed to be a constant and equal to 2×10^5 which has been adopted in many modeling exercises and fits well with field measurements (Mackay et al., 1986; Jurado et al., 2005; Fang et al., 2015; Li et al., 2017).

3 Results and discussion

3.1 Model evaluation and compared to observation

In order to better understand the variation, characteristics, and source contributions of the BC concentrations at Muztagh Ata Mountain, model sensitive studies using MOZART-4 were conducted in this study. Firstly, the model was evaluated by comparing the observed monthly BC concentrations with the calculated monthly BC concentrations during January 2004 to February 2006. As shown in Fig 3a, the simulated BC concentrations had a similar magnitude of measured BC concentrations, with mean values of 62.4 ng m^{-3} and 56.5 ng m^{-3} for the calculation and measurement, respectively. There was also evident that the measured variability of BC was captured by the calculation. For example, the calculated variability was comparable to the

measured result between July 2014 and Oct. 2015. However, some differences were also noticeable. For example, the calculated BC concentration was overestimated in the spring and winter of 2004 and underestimated in the winter of 2006. Because the measured site locates in a "clean" region of BC emission, the BC particles were mostly transported from long-distance of the upwind regions. There were uncertainty related to the emissions and simulated meteorological parameters (wind speeds, wind directions, etc.). As a result, it caused the discrepancy between calculated and measured BC concentrations at the Muztagh Ata Mountain. There was another reason may cause the difficulty of the calculation. The horizontal resolution of the global model is relatively low (1.9°×2.5° in this study), which is unable to reproduce some detailed variability in the simulation. However, the overall features of the measured BC concentrations were reproduced by the model, such as the magnitude and seasonal variability (see Fig. 3b), suggesting that the model is capable to study long-range transport from BC source regions to the remote site.

The simulated seasonal variation shows in Fig 3b. The result shows that calculated seasonal variation was generally agreed with the measured variation, except the value in spring. According to the analysis of the source contribution (shown in Section 3.3), the BC emission in South Asia has significant contributions to the BC concentrations at Muztagh Ata during non-summer season which accounted for average 31~60% in spring and few contributions in summer season. The overestimated BC concentrations may due to the fact that the model overestimated the pollutant transportation from the emission sources to sampling site crossing the high mountains of Tibet Plateau, which act as a wall to block the transportation from the BC emission in South Asia to the sampling area (Zhao et al., 2013).

3.2 Long-term Ice core measurement and possible effect of Kuwait fire event

In addition to the atmospheric sampling of BC measurement, there is a long-term ice cores measurement of BC at the Muztagh Ata Mountain. This long-term measurement represents a valuable data to show the long-term trend and inter-annual variability. Ice core records obtained at Muztagh Ata Mountain are irreplaceable when evaluating contemporary atmospheric or snow BC concentration variations. A long-term ice-core measurement (from 1940 to 2010) was provided by Xu et al. at Muztagh Ata

Mountain. Their results showed that the ice core BC concentrations were between 0.30 and 39.54 ng g^{-1} from 1940 to 2010, with an average value of 7.22 ng g^{-1}. The BC deposition fluxes were between 9.96 and 909.88 ng cm^{-2}, with an average of 184.18 ng cm^{-2}. It is interesting to note that both BC concentration and BC deposition of ice core showed a sharply increase in 1992, which was about five times higher than the average mean value as shown in Fig 4. No other similar peak was found in the entire record which may indicate a specific event to lead to this sharp increased, which provide useful information to track the BC emissions. In this study, we conduct several model studies to investigate this special event.

As shown in Figure 4, there was a high BC deposition flux (900 ng cm^{-2}) in 1992, compared to 100-300 ng cm^{-2} in other years. In order to investigate this special event, we focus our model study on a short period (from 1986 to 1994). One potential reason to cause this sharp increase of BC was that during 1991, when Iraqi troops withdrew from Kuwait at the end of the first Gulf War, they setted a huge fire over 700 oil wells. The fires were started in January and February 1991, and the last well was capped on November 6, 1991. The resulting fires produced a large plume of smoke and particles that had significant effects on the Persian Gulf area and the potential for global effects (as shown in Fig. 5).

In order to estimate intensive of the BC emission from the fires, Hobbs and Radke (1992) conducted two aircraft studies during the period 16 May through 12 June 1991 to evaluate the effects of the smoke. The estimated emission rate of elemental carbon of the Kuwait fires is ~3400 metric tons per day which is 13 times the BC emissions from all U.S. combustion sources in total.

In order to study the effect of the huge Kuwait fires on the BC ice core deposition, the MOZART-4 model was applied to simulate the atmospheric BC concentrations and deposition fluxes variation from 1986 to 1994. Several model sensitive studies were conducted. First, the atmospheric BC concentration was calculated by the anthropogenic BC emission with the default emissions (POET) as described before. Second, in order to simulate the large increase in the BC emissions caused by the Kuwait fires in Persian Gulf (Region 3 in Fig. 1), according to the measured values of Hobbs and Radke (1992), the BC emissions were significantly enhanced by 50 times

from January to November, 1991 to represent Kuwait fires. Figure 4 shows the horizontal distribution of the calculated BC plume from the Kuwait fires, with the enhanced BC emission.

The calculated result suggests that there was a significant increase of BC concentrations nearby the Kuwait fires (see Fig. 6). The BC concentrations reached to 10-20 $\mu g\ m^{-3}$ at the surface (see Fig. 6A) and more than 0.7 $\mu g\ m^{-3}$ at 5 km above the surface (see Fig. 6B). As shown in Figs. 5 and 6, the winds nearby the fire region were toward to northern and northwestern directions. Because the lifetime of black carbon aerosols is sufficiently long (about a week) (Ramanathan et al., 2001; Bauer et al., 2013), the high BC concentrations were transported westerly toward the Muztagh Ata Mountain.

The evaluation of the modeled BC deposition at the Muztagh Ata Mountain was conducted by comparison between the calculation and measurement (see Fig. 4). Figure 4 shows the calculated temporal variation of BC concentrations and deposition, which were compared with the measured variations. The result shows that the calculated temporal variability of BC deposition was generally consistent with the measured variability. For example, the both high peaks of calculated and measured BC deposition occurred in 1992. The calculated atmospheric concentrations of BC, however, had a peak value in 1991. This was due to the fact that the deposition of BC in ice core was an accumulated value, while the atmospheric BC concentration was an in-situ value. Despite of the consistence of temporal variations between measured and calculated deposition of BC, there was a consistent underestimate of calculated BC deposition compared to the measured value. Because there were uncertainties in estimates BC emission and the deposition, these uncertainties could result in the discrepancy between the calculation and measurement. For example, according to the assimilation meteorological data by Chinese Meteorological Admiration, the annual precipitation in 1992 was about twice higher than in 1991 nearby Muztagh Ata Mountain, suggesting that scavenging efficiency may likely underestimated, causing the calculated uncertainty in the estimate of the BC deposition.

3.3 Effect of regional BC emissions at the Muztagh Ata Mountain

To further understand the influence of transportation and deposition on the annual variation of BC at the Muztagh Ata Mountain (as a receptor region), sensitivity experiments using the MOZART-4 model were conducted. In the sensitive study, the effect of different BC emission regions on the BC concentrations at the measurement site was individually calculated. Four primary regions were defined with latitude and longitude as shown in Table 1 and Fig. 1, including (R1) Central Asia, (R2) Europe, (R3) Persian Gulf, and (R4) South Asia. Central Asia, Europe and South Asia previously have been reported as significant BC emission sources of Muztagh Ata Mountain (Liu et al., 2008; Xu et al., 2009a; Wang et al., 2015b). Europe is one of the biggest emission sources of the world located in the upwind region of receptor site although it is far away. Central Asia and South Asia are surrounding emission sources of the receptor site. Persian Gulf could be a potentially emission source which could be overlooked before. In each sensitive study, only the individual BC emission was included, and the BC emissions in other regions were excluded. As a result, the fractional contributions by the individual emission regions to BC concentrations in the receptor region (the Muztagh Ata Mountain) were calculated. Table 1 shows the calculated results.

In order to clearly show the transport pathways from the different regions to the measurement site and the Tibetan Plateau, the calculated horizontal distributions of BC concentrations from each region during 3 different periods (summer monsoon, non-monsoon, and annual mean) were shown in Fig. 7.

The results from Table 1 and Fig. 7 suggests that during the "normal period" (non Kuwait Fires), the BC emissions from Central Asia and South Asia had the largest contributions to the BC concentrations at measurement site, contributing annual mean of 27% and 25%, respectively. It is interesting to note that there were strong seasonal variations regarding the effects. During the monsoon period, the largest effect was due to the Central Asia source (44%), while during non-monsoon period, the largest effect was due to the South Asia source (34%).

As shown in Fig. 7, during the monsoon period, the airflow from the oceans (Persian Gulf and Bengal Bay) moves northward and coupled with the strong precipitation. As a result, the BC particles from south Asian source were washout during the

transport pathway, leading to lower BC concentrations at the measurement site. In contrast, during the non-monsoon period, the prevailing winds were western winds, which BC emission in the northern India was transported to the measurement site measurement site, leading to higher BC concentrations. The contributions from Persian Gulf emissions were generally low to the BC concentrations. However during Kuwait fires period, this region had significant contribution to the Muztagh Ata area as well as the Tibetan Plateau.

3.4 Radiative forcing induced by BC in Muztagh Ata glacier

The deposition of BC on the snow reduces the surface albedo, causing a positive radiative forcing and increases in ice and snow melt. Previous studies show that BC particles produce significant reduction in the snow albedo, with the solar visible wavelengths (Warren and Wiscombe, 1980). In this study, the effect of BC deposition on the snow albedo and radiative forcing during 1986 to 1994 in Muztagh Ata glacier was estimated. The SINICAR model (Snow, Ice, and Aerosol Radiation; available at http://snow.engin.umich.edu) was used to estimate the effect of BC particles on snow albedo in different solar wavelengths (Flanner and Zender, 2005; Flanner et al., 2007).

To estimate the effect of the BC deposition on surface albedo, in addition to the BC concentrations, there are several environmental factors such as snow grain size, solar zenith angle, and snow depth were needed to be estimated (Warren and Wiscombe, 1980). The setup of input parameters required for running the SNICAR model is briefly described as below. As we focus on the calculation of radiative forcing caused by BC particles, other impurity contents, such as dust and volcanic ash, were set to be zero. A mass absorption cross section (MAC) of 7.5 m^2 g^{-1} at 550 nm for uncoated BC particles (Bond and Bergstrom, 2006) was assumed to be same as the default value, and the MAC scaling factor in the online SNICAR model as one of input parameters was set to be 1.0. The effective radius of 100 μm with a density of 60 kg m^{-3} was used for new snow, and the effective radius of 400 μm with a density of 400 kg m^{-3} was adopted for the albedo estimation according to the previous studies and measurements in other studies in Tibetan Plateau (Wiscombe and Warren, 1980; Wu et al., 2006). The extractive snow height from MERRA (the Modern-Era Retrospective-analysis for Research and Applications) reanalysis products was used for snowpack thickness. The

forcing dataset used in this study was developed by Data Assimilation and Modeling Center for Tibetan Multi-spheres, Institute of Tibetan Plateau Research, Chinese Academy of Sciences (Chen et al., 2011). The recovered BC concentrations of ice core were used as the input parameter of uncoated black carbon concentration. The averaged short-wave flux and solar zenith angle of each month were obtained from China Meteorological Forcing Dataset provided by Data Assimilation and Modeling Center for Tibetan Multi-spheres, Institute of Tibetan Plateau Research, Chinese Academy of Sciences.

The measured average BC concentration in ice core during 1986-1994 was 15.2 ng g^{-1}, with a peak value of 39.2 ng g^{-1}. The calculated snow albedo reduction by using the SNICAR model ranged from 0.11% to 1.36% by assuming that the snow layer was totally covered by fresh snow (lower limit). However, if it was aged layer, the estimated snow albedo reduction increased, ranging from 0.47% to 2.97% (upper limit). The actual value should be lied between the two ranges. This result is consistent with the previous studies. For example, (Yasunari et al., 2010) reported that the reduction of snow albedo ranged from 2.0% to 5.2%, with the BC concentration of 26.0-68.2 ng/g, based on atmospheric BC measurements at NCO-P over the southern slopes of western Himalayas.

The reduction of snow albedo enhanced the absorption of solar energy and accelerated snow and ice melt (Conway et al., 1996). Several studies suggested that that BC containments on snow were very effective to reduce the surface albedo (Warren and Wiscombe, 1980; Petr Chylek and Srivastava, 1983; Gardner and Sharp, 2010). In this study, the effects of BC containments on snow albedo and snow water equivalent (SWE) reduction were estimated.

Figure 8 shows the calculated the effects of BC containments on annual mean radiative forcing increase (RFI) (W m^{-2}) and snow water equivalent (SWE) reduction (mm yr^{-1}; millimeter per year), under fresh snow assumption and aged snow assumption. The results show that under the fresh snow assumption (lower limit), the increases of RFI ranged from 0.2 W m^{-2} to 2.5 W m^{-2}, while under the aged snow assumption (upper limit), the increases of RFI ranged from 0.9 W m^{-2} to 5.7 W m^{-2}.

This estimate is consistent with the previous studies (Flanner et al., 2009)During the Kuwait fires period, the RFI values increased about 2-5 times higher, which led to a significant increase for the snow melting during the period.

The potential influence for BC deposition on glaciers from forest fires was highlighted that was coincident with an increase discharge in the downriver in previous study (Kaspari et al., 2015). The runoff of the melted snow due to the increase of snow surface albedo was estimated in this study. A first-order estimation was based on the additional energy contribution to the snowpack due to BC deposition. First the melting point of snow was estimated. Second, the extra snow melt from light absorbing black carbon was estimated by dividing hourly instantaneous radiative forcing, with the enthalpy of fusion of water at 0 ^{o}C of 0.334 $\times 10^{6}$ J kg^{-1} (Painter et al., 2013; Kaspari et al., 2015). The estimation represented the snow melt in kg m^{-2} across the hour during acquisition translates, or melt in mm of snow water equivalent (SWE). The melted snow due to the BC water was calculated (shown in Fig. 8). The result shows that the estimated averaged SWE reductions were 111 mm and 270 mm, for fresh and aged snow respectively. During the Kuwait fires period, the estimated SWE significantly increased, reaching to 600 mm for aged snow condition, and 300 mm for fresh snow condition. The increase was about 3 times than pre- and post-Kuwait fires, suggesting that this special event had a significant impact on snow melting for the Tibetan glaciers and the water resources in the region. However, this estimate of runoff is speculative since there are a number of influential factors. Schmale et al. (2017) found that combination effect of meteorological parameters and snow albedo could be 3 times larger than model results. The Tibetan Plateau is recognized as “Water Tower of Asia” with largely contribution to annual river discharge of Yangtze River, Indus and Brahmaputra etc. The snowmelt runoff will impact on regional climate system including the timing of runoff, the frequency and intensity of floods and rainfall patterns because of its tightening interactive with the hydrologic cycle (Jain et al., 2010). Wu and Qian (2003) reported that Tibetan winter snow cover is abnormally linked to rainfall over south, southeast and east Asia by observation data analysis.

4 Conclusions

Black carbon (BC) particles change the radiative balance of the atmosphere by absorbing and scattering solar radiation. As a result, BC deposition on the surface of snow and ice changes the albedo of solar radiation. Albedo change is the key parameter to affect the melting of glacier in Tibetan Plateau. In order to study this effect, two sets of measurements were used to study the variability of BC deposition at Muztagh Ata Mountain, Northern Tibetan Plateau. The measured data included the air samplings of BC particles during 2004-2006 and the ice core drillings of BC deposition during 1986-1994. To identify the effect of BC emissions on the BC deposition in this region, a global chemical transportation model (MOZART-4) was used to analyze the BC transport from the source regions. A radiative transfer model (SNICAR) was used to study the effect of BC deposition on snow albedo.

The results show some important highlights to reveal the temporal variability of BC deposition and the effect of long-rang transport on the BC pollution in the Northern Tibetan Plateau, which are summarized as the follows;

(1) During 1991-1992, there was a strong spike of the BC deposition at Muztagh Ata, suggesting that there was unusual emission in the upward region. This high peak of BC deposition was investigated by using the global chemical transportation model (MOZART-4). The analysis indicated that the emissions from large Kuwait fires at the end of the first Gulf War in 1991 caused the high peak of the BC concentrations and the BC deposition. As a result, the BC deposition in 1991 and 1992 at the Muztagh Ata Mountain was 3-4 times higher than other periods.

(2) The effect of Kuwait fires on the BC deposition at the Muztagh Ata Mountain suggested that the upward BC emissions had important impacts on this remote site located in Northern Tibetan Plateau. In order to quantitatively estimate the effect of surrounding emissions on the BC concentrations in the northern Tibetan Plateau, a sensitive study with 4 individual BC emission regions (Central Asia, Europe, Persian Gulf, and South Asia) was conducted by using the MOZART-4 model. The result suggests that during the “normal period” (non Kuwait Fires), the largest effect was due to the Central Asia source (44%) during Indian monsoon period. During non-monsoon period, the largest effect

was due to the South Asia source (34%).

(3) The increase of radiative forcing increase (RFI) due to the deposition of BC on snow was estimated by using the radiative transfer model (SNICAR). The results show that under the fresh snow assumption, the estimated RFI ranged from 0.2 W m^{-2} to 2.5 W m^{-2}, while under the aged snow assumption, the estimated RFI ranged from 0.9 W m^{-2} to 5.7 W m^{-2}. During the Kuwait fires period, the RFI values increased about 2-5 times higher than the "normal period", suggesting a significant increase for the snow melting in Northern Tibetan Plateau due to this fire event.

This result suggests that the variability of BC deposition at the Muztagh Ata Mountain provides useful information to study the effect of the upward BC emissions on environmental and climate issues in the Northern Tibetan Plateau. The radiative effect of BC deposition on the snow melting provides important information regarding the water resources in the region.

Acknowledgement

This work was supported by the National Natural Science Foundation of China (NSFC) under Grant Nos. 41430424, 41730108 and 41230641. The Authors thanks the supports of Center for Excellence in Urban Atmospheric Environment, Institute of Urban Environment, Chinese Academy of Sciences. The National Center for Atmospheric Research is sponsored by the National Science Foundation.

References

An, Z. S., Kutzbach, J. E., Prell, W. L., and Porter, S. C.: Evolution of Asian monsoons and phased uplift of the Himalaya-Tibetan plateau since Late Miocene times, Nature, 411, 62–66, doi:10.1038/35075035, 2001.

Bauer, S. E., Bausch, A., Nazarenko, L., Tsigaridis, K., Xu, B., Edwards, R., Bisiaux, M., and McConnell, J.: Historical and future black carbon deposition on the three ice caps: Ice core measurements and model simulations from 1850 to 2100, J. Geophys. Res. Atmos., 118, 7948–7961, doi:10.1002/jgrd.50612, 2013.

Bisiaux, M. M., Edwards, R., McConnell, J. R., Curran, M. A. J., van Ommen, T. D., Smith, A. M., Neumann, T. A., Pasteris, D. R., Penner, J. E., and Taylor, K.: Changes in black carbon deposition to Antarctica from two high-resolution ice core records, 1850–2000 AD, Atmos. Chem. Phys., 12, 4107–4115, doi:10.5194/acp-12-4107-2012, 2012.

Bond, T. C. and Bergstrom, R. W.: Light Absorption by Carbonaceous Particles: An Investigative Review, Aerosol Sci. Tech., 40, 27–67, doi:10.1080/02786820500421521, 2006.

Bond, T. C., Streets, D. G., Yarber, K. F., Nelson, S. M., Woo, J.-H., and Klimont, Z.: A technology-based global inventory of black and organic carbon emissions from combustion, J. Geophys. Res., 109, 1042, doi:10.1029/2003JD003697, 2004.

Brasseur, G. P., Hauglustaine, D. A., Walters, S., Rasch, P. J., Müller, J.-F., Granier, C., and Tie, X. X.: MOZART, a global chemical transport model for ozone and related chemical tracers: 1. Model description, J. Geophys. Res., 103, 28265–28289, doi:10.1029/98JD02397, 1998.

Cao, J. J., Lee, S. C., Ho, K. F., Zhang, X. Y., Zou, S. C., Fung, K., Chow, J. C., and Watson, J. G.: Characteristics of carbonaceous aerosol in Pearl River Delta Region, China during 2001 winter period, Atmos. Environ., 37, 1451–1460, doi:10.1016/S1352-2310(02)01002-6, 2003.

Cao, J. J., Xu, B. Q., He, J. Q., Liu, X. Q., Han, Y. M., Wang, G. H., and Zhu, C. S.: Concentrations, seasonal variations, and transport of carbonaceous aerosols at a remote Mountainous region in western China, Atmos. Environ., 43, 4444–4452, 2009.

Chang, L. Y., Xu, J. M., Tie, X. X., and Wu, J. B.: Impact of the 2015 El Nino event on winter air quality in China, Sci. Rep., 6, 34275, doi:10.1038/srep34275, 2016.

Chen, Y., Yang, K., He, J., Qin, J., Shi, J., Du, J., and He, Q.: Improving land surface temperature modeling for dry land of China, J. Geophys. Res., 116, 251, doi:10.1029/2011JD015921, 2011.

Chow, J. C., Watson, J. G., Chen, L. W. A., Arnott, W. P., Moosmüller, H., and Fung, K.: Equivalence of elemental carbon by thermal/optical reflectance and transmittance with different temperature protocols, Environ. Sci. Technol., 38, 4414–4422, 2004.

Chow, J. C., Watson, J. G., Pritchett, L. C., Pierson, W. R., Frazier, C. A., and Purcell, R. G.: The dri thermal/optical reflectance carbon analysis system: Description,

evaluation and applications in U.S. Air quality studies, Atmos. Environ. Part A. General Topics., 27, 1185–1201, doi:10.1016/0960-1686(93)90245-T, 1993.
Conway, H., Gades, A., and Raymond, C. F.: Albedo of dirty snow during conditions of melt, Water Resour. Res., 32, 1713–1718, doi:10.1029/96WR00712, 1996.
Cooke, W. F. and Wilson, J. J. N.: A global black carbon aerosol model, J. Geophys. Res., 101, 19395–19409, doi:10.1029/96JD00671, 1996.
Emmons, L. K., Walters, S., Hess, P. G., Lamarque, J.-F., Pfister, G. G., Fillmore, D., Granier, C., Guenther, A., Kinnison, D., Laepple, T., Orlando, J., Tie, X., Tyndall, G., Wiedinmyer, C., Baughcum, S. L., and Kloster, S.: Description and evaluation of the Model for Ozone and Related chemical Tracers, version 4 (MOZART-4), Geosci. Model Dev., 3, 43–67, doi:10.5194/gmd-3-43-2010, 2010.
Fang, Y., Chen, Y. J., Tian, C. G., Lin, T., Hu, L. M., Huang, G. P., Tang, J. H., Li, J., and Zhang, G.: Flux and budget of BC in the continental shelf seas adjacent to Chinese high BC emission source regions, Global Biogeochem. Cycles, 29, 957–972, doi:10.1002/2014GB004985, 2015.
Flanner, M. G. and Zender, C. S.: Snowpack radiative heating: Influence on Tibetan Plateau climate, Geophys. Res. Lett., 32, 10,219, doi:10.1029/2004GL022076, 2005.
Flanner, M. G., Zender, C. S., Hess, P. G., Mahowald, N. M., Painter, T. H., Ramanathan, V., and Rasch, P. J.: Springtime warming and reduced snow cover from carbonaceous particles, Atmos. Chem. Phys., 9, 2481–2497, doi:10.5194/acp-9-2481-2009, 2009.
Flanner, M. G., Zender, C. S., Randerson, J. T., and Rasch, P. J.: Present-day climate forcing and response from black carbon in snow, J. Geophys. Res., 112, 3131, doi:10.1029/2006JD008003, 2007.
Gardner, A. S. and Sharp, M. J.: A review of snow and ice albedo and the development of a new physically based broadband albedo parameterization, J. Geophys. Res., 115, D13203, doi:10.1029/2009JF001444, 2010.
Hack, J. J.: Parameterization of moist convection in the National Center for Atmospheric Research community climate model (CCM2), J. Geophys. Res., 99, 5551, doi:10.1029/93JD03478, 1994.
Hagen, D. E., Trueblood, M. B., and Whitefield, P. D.: A Field Sampling of Jet Exhaust Aerosols, Particulate Sc. & Tech., 10, 53–63, doi:10.1080/02726359208906598, 1992.
Hansen, J. and Nazarenko, L.: Soot climate forcing via snow and ice albedos, P. Natl. Acad. Sci. USA, 101, 423–428, 2004.
Hobbs, P. V. and Radke, L. F.: Airborne studies of the smoke from the kuwait oil fires, Science, 256, 987–991, doi:10.1126/science.256.5059.987, 1992.
Holben, B. N., Eck, T. F., Slutsker, I., Tanré, D., Buis, J. P., Setzer, A., Vermote, E., Reagan, J. A., Kaufman, Y. J., Nakajima, T., Lavenu, F., Jankowiak, I., and Smirnov, A.: AERONET—A Federated Instrument Network and Data Archive for Aerosol Characterization, Remote Sens. Environ., 66, 1–16, doi:10.1016/S0034-4257(98)00031-5, 1998.
Holtslag, A. A. M. and Boville, B. A.: Local Versus Nonlocal Boundary-Layer

Diffusion in a Global Climate Model, J. Climate, 6, 1825–1842, doi:10.1175/1520-0442(1993)006<1825:LVNBLD>2.0.CO;2, 1993.
Jain, S. K., Goswami, A., and Saraf, A. K.: Assessment of Snowmelt Runoff Using Remote Sensing and Effect of Climate Change on Runoff, Water Resour Manage, 24, 1763–1777, doi:10.1007/s11269-009-9523-1, 2010.
Jurado, E., Dachs, J., Duarte, C. M., and Simó, R.: Atmospheric deposition of organic and black carbon to the global oceans, Atmos. Environ., 42, 7931–7939, doi:10.1016/j.atmosenv.2008.07.029, 2008.
Jurado, E., Jaward, F., Lohmann, R., Jones, K. C., Simó, R., and Dachs, J.: Wet Deposition of Persistent Organic Pollutants to the Global Oceans, Environ. Sci. Technol., 39, 2426–2435, doi:10.1021/es048599g, 2005.
Kaspari, S., McKenzie Skiles, S., Delaney, I., Dixon, D., and Painter, T. H.: Accelerated glacier melt on Snow Dome, Mount Olympus, Washington, USA, due to deposition of black carbon and mineral dust from wildfire, J. Geophys. Res. Atmos., 120, 2793–2807, doi:10.1002/2014JD022676, 2015.
Kaspari, S. D., Schwikowski, M., Gysel, M., Flanner, M. G., Kang, S., Hou, S., and Mayewski, P. A.: Recent increase in black carbon concentrations from a Mt. Everest ice core spanning 1860-2000 AD, Geophys. Res. Lett., 38, n/a-n/a, doi:10.1029/2010GL046096, 2011.
Kinnison, D. E., Brasseur, G. P., Walters, S., Garcia, R. R., Marsh, D. R., Sassi, F., Harvey, V. L., Randall, C. E., Emmons, L., Lamarque, J. F., Hess, P., Orlando, J. J., Tie, X. X., Randel, W., Pan, L. L., Gettelman, A., Granier, C., Diehl, T., Niemeier, U., and Simmons, A. J.: Sensitivity of chemical tracers to meteorological parameters in the MOZART-3 chemical transport model, J. Geophys. Res., 112, 32295, doi:10.1029/2006JD007879, 2007.
Lavanchy, V.M.H., Gäggeler, H. W., Schotterer, U., Schwikowski, M., and Baltensperger, U.: Historical record of carbonaceous particle concentrations from a European high-alpine glacier (Colle Gnifetti, Switzerland), J. Aerosol Sci., 30, S611-S612, doi:10.1016/S0021-8502(99)80316-4, 1999.
Li, C. L., Yan, F. P., Kang, S. C., Chen, P. F., Han, X. W., Hu, Z. F., Zhang, G. S., Hong, Y., Gao, S. P., Qu, B., Zhu, Z. J., Li, J. W., Chen, B., and Sillanpää, M.: Re-evaluating black carbon in the Himalayas and the Tibetan Plateau: Concentrations and deposition, Atmos. Chem. Phys., 17, 11899–11912, doi:10.5194/acp-17-11899-2017, 2017.
Lin, S.-J. and Rood, R. B.: Multidimensional Flux-Form Semi-Lagrangian Transport Schemes, Mon. Wea. Rev., 124, 2046–2070, doi:10.1175/1520-0493(1996)124<2046:MFFSLT>2.0.CO;2, 1996.
Liousse, C., Cachier, H., and Jennings, S. G.: Optical and thermal measurements of black carbon aerosol content in different environments: Variation of the specific attenuation cross-section, sigma (σ), Atmospheric Environment. Part A. General Topics, 27, 1203–1211, doi:10.1016/0960-1686(93)90246-U, 1993.
Liu, X. Q., Xu, B. Q., Yao, T. D., Wang, N. L., and Wu, G. J.: Carbonaceous particles in Muztagh Ata ice core, West Kunlun Mountains, China, Sci. Bull., 53, 3379–3386, doi:10.1007/s11434-008-0294-5, 2008.

712 Mackay, D., Paterson, S., and Schroeder, W. H.: Model describing the rates of transfer
713 processes of organic chemicals between atmosphere and water, Environ. Sci.
714 Technol., 20, 810–816, doi:10.1021/es00150a009, 1986.
715 McConnell, J. R., Edwards, R., Kok, G. L., Flanner, M. G., Zender, C. S., Saltzman, E.
716 S., Banta, J. R., Pasteris, D. R., Carter, M. M., and Kahl, J. D. W.: 20th-century
717 industrial black carbon emissions altered Arctic climate forcing, Science, 317,
718 1381–1384, doi:10.1126/science.1144856, 2007.
719 Ming, J., Cachier, H., Xiao, C., Qin, D., Kang, S., Hou, S., and Xu, J.: Black carbon
720 record based on a shallow Himalayan ice core and its climatic implications, Atmos.
721 Chem. Phys., 8, 1343–1352, doi:10.5194/acp-8-1343-2008, 2008.
722 Nair, V. S., Babu, S. S., Moorthy, K. K., Sharma, A. K., Marinoni, A., and Ajai: Black
723 carbon aerosols over the Himalayas: Direct and surface albedo forcing, Tellus B,
724 65, 19738, doi:10.3402/tellusb.v65i0.19738, 2013.
725 Painter, T. H., Seidel, F. C., Bryant, A. C., McKenzie Skiles, S., and Rittger, K.:
726 Imaging spectroscopy of albedo and radiative forcing by light-absorbing
727 impurities in mountain snow, J. Geophys. Res. Atmos., 118, 9511–9523,
728 doi:10.1002/jgrd.50520, 2013.
729 Parungo, F., Nagamoto, C., Zhou, M.-Y., Hansen, A. D.A., and Harris, J.: Aeolian
730 transport of aerosol black carbon from Aeolian transport of aerosol black carbon
731 from China to the ocean, Atmos. Environ., 28, 3251–3260, 1994.
732 Petr Chylek, V. R. and Srivastava, V.: Albedo of soot-contaminated snow, J. Geophys.
733 Res., 88, 10837–10843, 1983.
734 Petzold, A., Ogren, J. A., Fiebig, M., Laj, P., Li, S.-M., Baltensperger, U.,
735 Holzer-Popp, T., Kinne, S., Pappalardo, G., Sugimoto, N., Wehrli, C.,
736 Wiedensohler, A., and Zhang, X.-Y.: Recommendations for reporting "black
737 carbon" measurements, Atmos. Chem. Phys., 13, 8365–8379,
738 doi:10.5194/acp-13-8365-2013, 2013.
739 Ramanathan, V., Crutzen, P. J., Kiehl, J. T., and Rosenfeld, D.: Aerosols, climate, and
740 the hydrological cycle, Science, 294, 2119–2124, 2001.
741 Rasch, P. J., Mahowald, N. M., and Eaton, B. E.: Representations of transport,
742 convection, and the hydrologic cycle in chemical transport models: Implications
743 for the modeling of short-lived and soluble species, J. Geophys. Res., 102,
744 28,127-28,138, 1997.
745 Schmale, J., Flanner, M., Kang, S., Sprenger, M., Zhang, Q., Guo, J., Li, Y.,
746 Schwikowski, M., and Farinotti, D.: Modulation of snow reflectance and
747 snowmelt from Central Asian glaciers by anthropogenic black carbon, Sci. Rep., 7,
748 40501, doi:10.1038/srep40501, 2017.
749 Schwarz, J. P., Gao, R. S., Fahey, D. W., Thomson, D. S., Watts, L. A., Wilson, J. C.,
750 Reeves, J. M., Darbeheshti, M., Baumgardner, D. G., Kok, G. L., Chung, S. H.,
751 Schulz, M., Hendricks, J., Lauer, A., Kärcher, B., Slowik, J. G., Rosenlof, K. H.,
752 Thompson, T. L., Langford, A. O., Loewenstein, M., and Aikin, K. C.:
753 Single-particle measurements of midlatitude black carbon and light-scattering
754 aerosols from the boundary layer to the lower stratosphere, J. Geophys. Res., 111,
755 2845, doi:10.1029/2006JD007076, 2006.

Tie, X. X., Madronich, S., Walters, S., Edwards, D. P., Ginoux, P., Mahowald, N., Zhang, R. Y., Lou, C., and Brasseur, G.: Assessment of the global impact of aerosols on tropospheric oxidants, J. Geophys. Res., 110, 13,791, doi:10.1029/2004JD005359, 2005.

Wang, M., Xu, B., Cao, J., Tie, X., Wang, H., Zhang, R., Qian, Y., Rasch, P. J., Zhao, S., Wu, G., Zhao, H., Joswiak, D. R., Li, J., and Xie, Y.: Carbonaceous aerosols recorded in a southeastern Tibetan glacier: Analysis of temporal variations and model estimates of sources and radiative forcing, Atmos. Chem. Phys., 15, 1191–1204, doi:10.5194/acp-15-1191-2015, 2015a.

Wang, M., Xu, B. Q., Kaspari, S. D., Gleixner, G., Schwab, V. F., Zhao, H. B., Wang, H. L., and Yao, P.: Century-long record of black carbon in an ice core from the Eastern Pamirs: Estimated contributions from biomass burning, Atmos. Environ., 115, 79–88, doi:10.1016/j.atmosenv.2015.05.034, 2015b.

Warren, S. G. and Wiscombe, W. J.: A Model for the Spectral Albedo of Snow. II: Snow Containing Atmospheric Aerosols, J. Atmos. Sci., 37, 2734–2745, doi:10.1175/1520-0469(1980)037<2734:AMFTSA>2.0.CO;2, 1980.

Wendl, I. A., Menking, J. A., Färber, R., Gysel, M., Kaspari, S. D., Laborde, M. J. G., and Schwikowski, M.: Optimized method for black carbon analysis in ice and snow using the Single Particle Soot Photometer, Atmos. Meas. Tech., 7, 2667–2681, doi:10.5194/amt-7-2667-2014, 2014.

Wiscombe, W. J. and Warren, S. G.: A Model for the Spectral Albedo of Snow. I: Pure Snow, J. Atmos. Sci., 37, 2712–2733, doi:10.1175/1520-0469(1980)037<2712:AMFTSA>2.0.CO;2, 1980.

Wu, G. J., Yao, T. D., Xu, B. Q., Li, Z., Tian, L. D., Duan, K. Q., and Wen, L. K.: Grain size record of microparticles in the Muztagata ice core, Sci. China Ser. D, 49, 10–17, doi:10.1007/s11430-004-5093-5, 2006.

Wu, G. J., Yao, T. D., Xu, B. Q., Tian, L. D., Li, Z., and Duan, K. Q.: Seasonal variations of dust record in the Muztagata ice cores, Sci. Bull., 53, 2506–2512, doi:10.1007/s11434-008-0197-5, 2008.

Wu, T. and Qian, Z.: The relation between the Tibetan winter snow and the Asian summer monsoon and rainfall: an observational investigation, Journal of Climate, 16, 2038–2051, 2003.

Xu, B., Cao, J., Hansen, J., Yao, T., Joswia, D. R., Wang, N., Wu, G., Wang, M., Zhao, H., Yang, W., Liu, X., and He, J.: Black soot and the survival of Tibetan glaciers, P. Natl. Acad. Sci. USA, 106, 22114–22118, doi:10.1073/pnas.0910444106, 2009a.

Xu, B. Q., Wang, M., Joswiak, D. R., Cao, J. J., Yao, T. D., Wu, G. J., Yang, W., and Zhao, H. B.: Deposition of anthropogenic aerosols in a southeastern Tibetan glacier, J. Geophys. Res., 114, 9185, doi:10.1029/2008JD011510, 2009b.

Yasunari, T. J., Bonasoni, P., Laj, P., Fujita, K., Vuillermoz, E., Marinoni, A., Cristofanelli, P., Duchi, R., Tartari, G., and Lau, K.-M.: Estimated impact of black carbon deposition during pre-monsoon season from Nepal Climate Observatory – Pyramid data and snow albedo changes over Himalayan glaciers, Atmos. Chem. Phys., 10, 6603–6615, doi:10.5194/acp-10-6603-2010, 2010.

Yasunari, T. J., Tan, Q., Lau, K.-M., Bonasoni, P., Marinoni, A., Laj, P., Ménégoz, M.,

Takemura, T., and Chin, M.: Estimated range of black carbon dry deposition and the related snow albedo reduction over Himalayan glaciers during dry pre-monsoon periods, Atmos. Environ., 78, 259–267, doi:10.1016/j.atmosenv.2012.03.031, 2013.

Zhang, G. J. and McFarlane, N. A.: Sensitivity of climate simulations to the parameterization of cumulus convection in the Canadian climate centre general circulation model, Atmos. Ocean, 33, 407–446, doi:10.1080/07055900.1995.9649539, 1995.

Zhao, H. B., Xu, B. Q., Yao, T. D., Tian, L. D., and Li, Z.: Records of sulfate and nitrate in an ice core from Mount Muztagata, central Asia, J. Geophys. Res., 116, 275, doi:10.1029/2011JD015735, 2011.

Zhao, Z., Cao, J., Shen, Z., Xu, B., Zhu, C., Chen, L.-W. A., Su, X., Liu, S., Han, Y., Wang, G., and Ho, K.: Aerosol particles at a high-altitude site on the Southeast Tibetan Plateau, China: Implications for pollution transport from South Asia, J. Geophys. Res. Atmos., 118, 11,360-11,375, doi:10.1002/jgrd.50599, 2013.

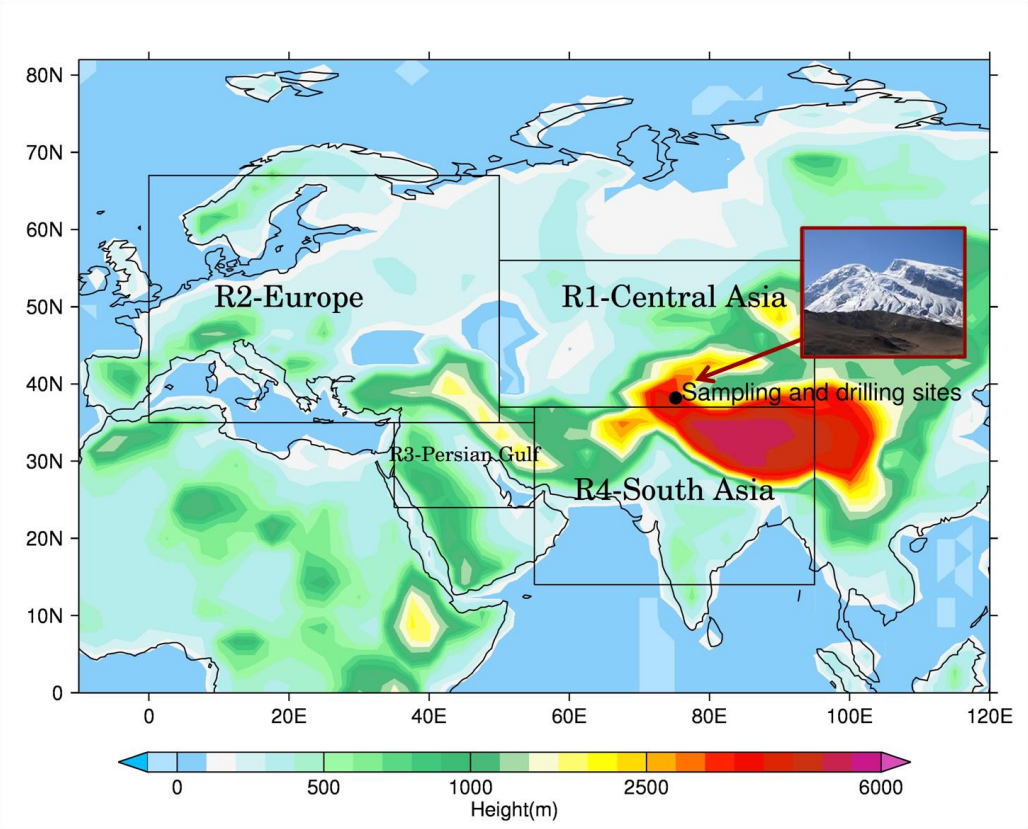

Fig 1. The Muztagh Ata measurement site (indicated by dot), and the surrounding BC source areas (R1-Central Asia region; R2-European region; R3-Persian Gulf region; and R4-South Asia region).

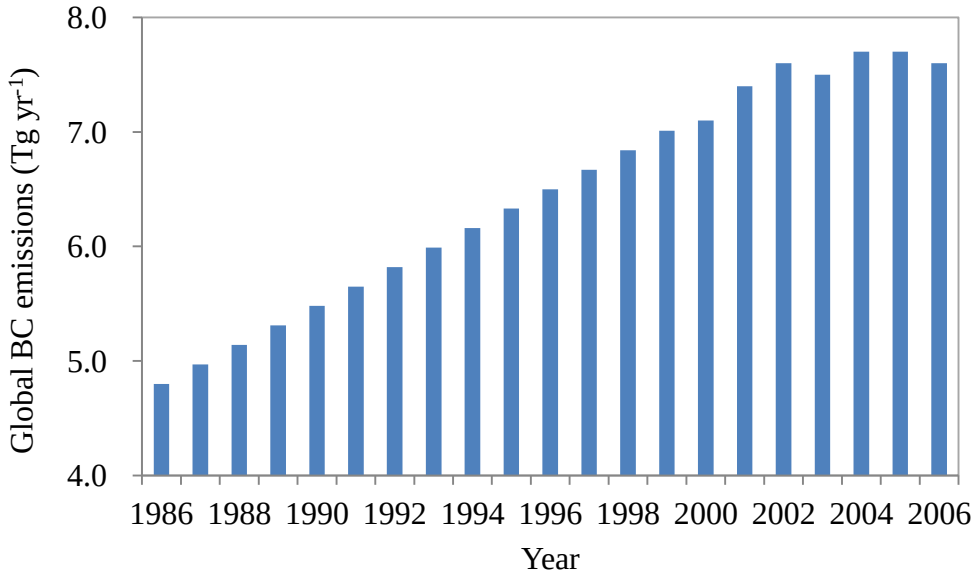

Fig 2. The trend of global BC emission (Tg/yr) from 1986 to 2006 used in this study

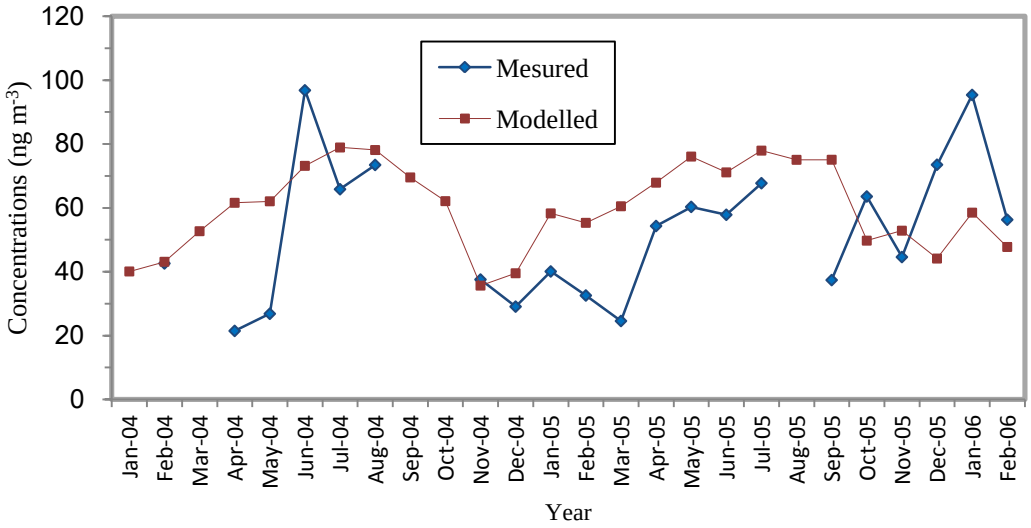

Fig 3a. Comparison of calculated (red) and measured (blue) monthly mean BC concentrations at the surface level during Jan. 2004 to Feb. 2006 measured by the Cold and Arid Regions Environmental and Engineering Institute, Chinese Academy of Sciences.

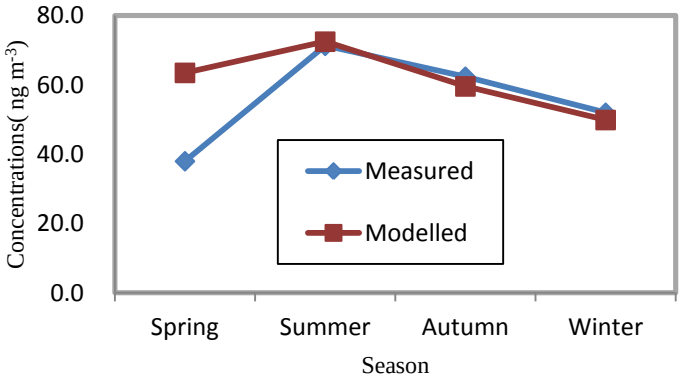

Fig 3b. Comparison of calculated (red) and measured (blue) seasonal variation during Jan. 2004 to Feb. 2006. Spring includes March, April and May in 2004 and 2005. Summer includes June, July and August in 2004, 2005; Autumn includes September, October and November in 2004, 2005; Winter includes December, January and February of 2004, 2005 and January, February in 2006.

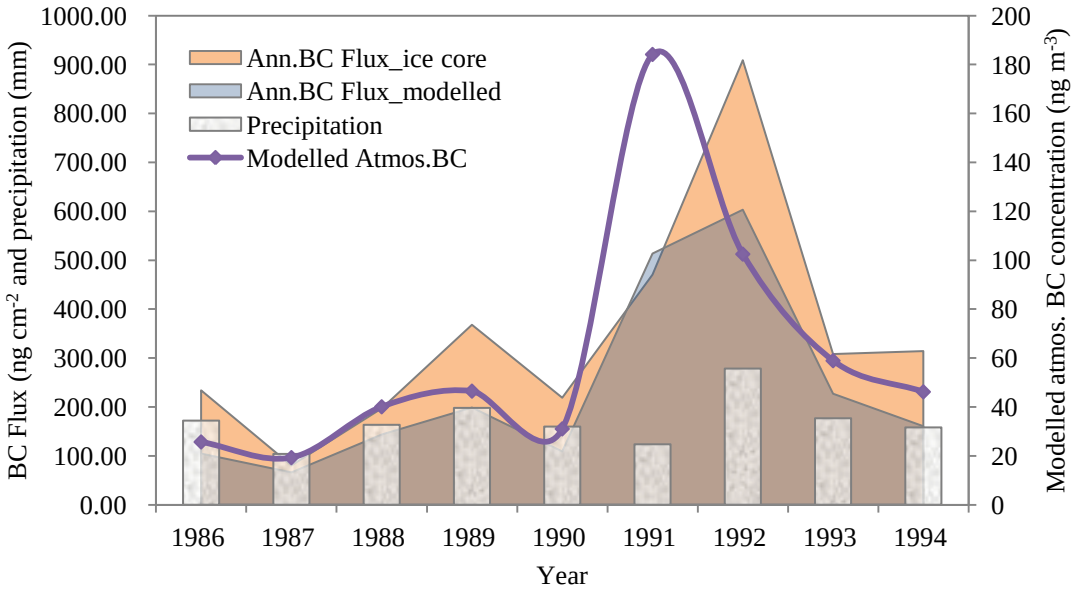

836

837 **Fig 4. Comparison of measured annual BC deposition flux with the model calculation between ice core and**
838 **simulation, as well as the modelled atmospheric BC concentration and precipitation used for BC deposition**
839 **flux calculation**

840

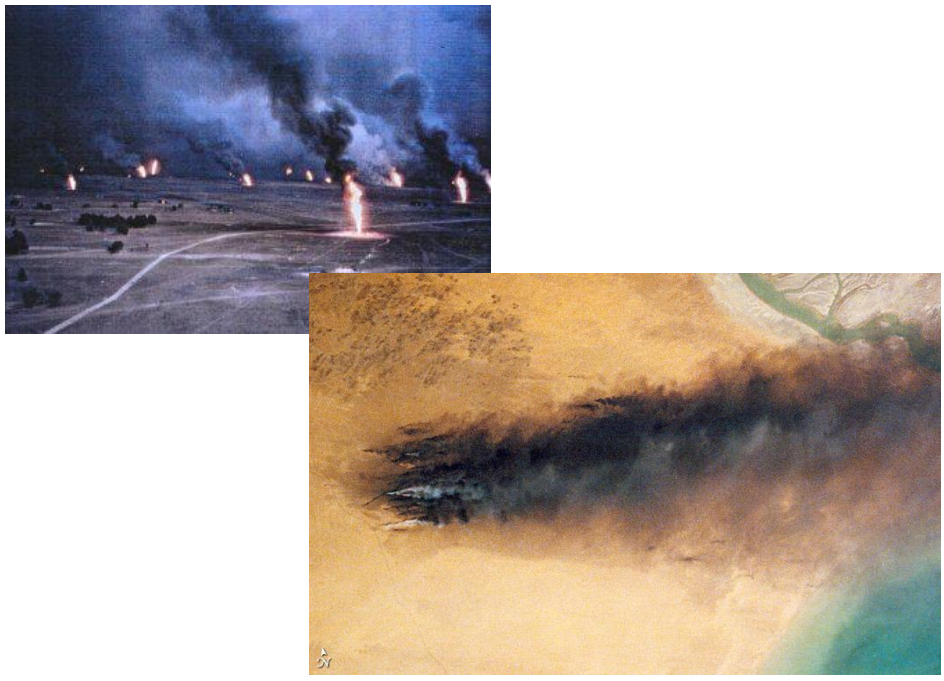

841

842 **Fig 5. The image of the fires in Kuwait during 1991. It shows the intensive fires and the raise up of plume**
843 **due to the heat buoyance. The lower panel shows the fires were transported to east due to western winds.**

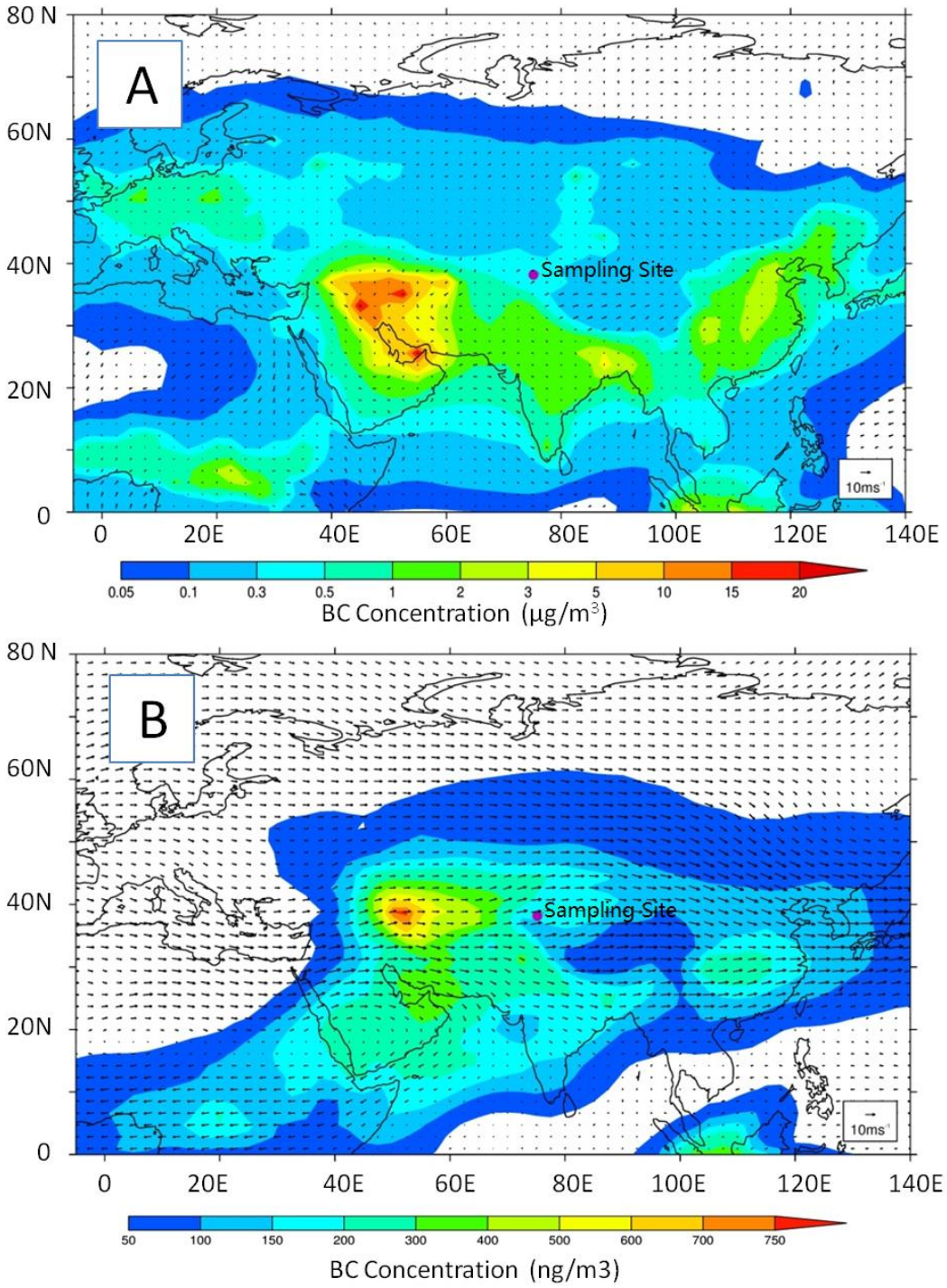

844

845 **Fig. 6. The calculated horizontal distributions of BC concentrations (μg m^{-3}) at the surface (A) and the**
846 **concentrations (ng m^{-3}) at 5 km above the surface (B) in Kuwait during 1991. The wind direction and speed**
847 **are indicated by black arrows.**

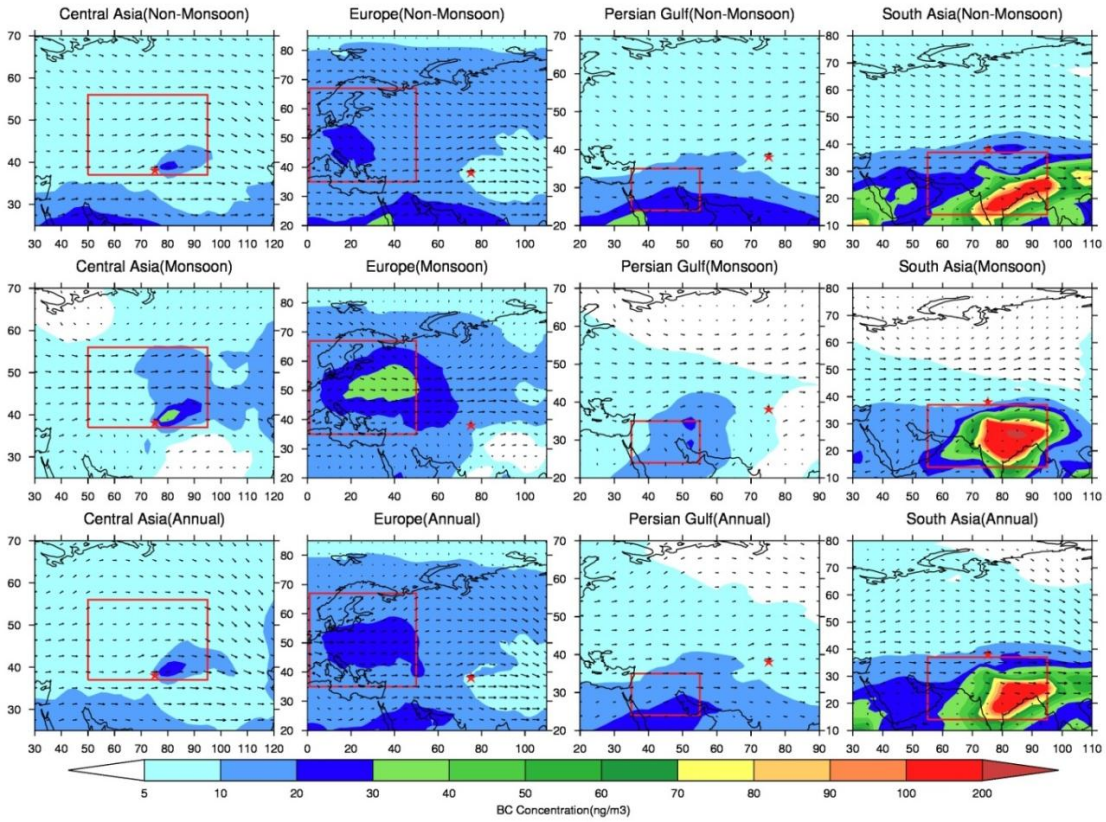

Fig 7. The calculated spatial BC distributions due to individual BC from the four source regions (Central Asia, Europe, Persian Gulf and South Asia) above 5 km above the surface during different periods, i.e., monsoon (June-September), non-monsoon (October-May), and annual mean in 1993. The red star is where the study site of Muztagh Ata located. The red boxes indicate the boundary of the four source regions.

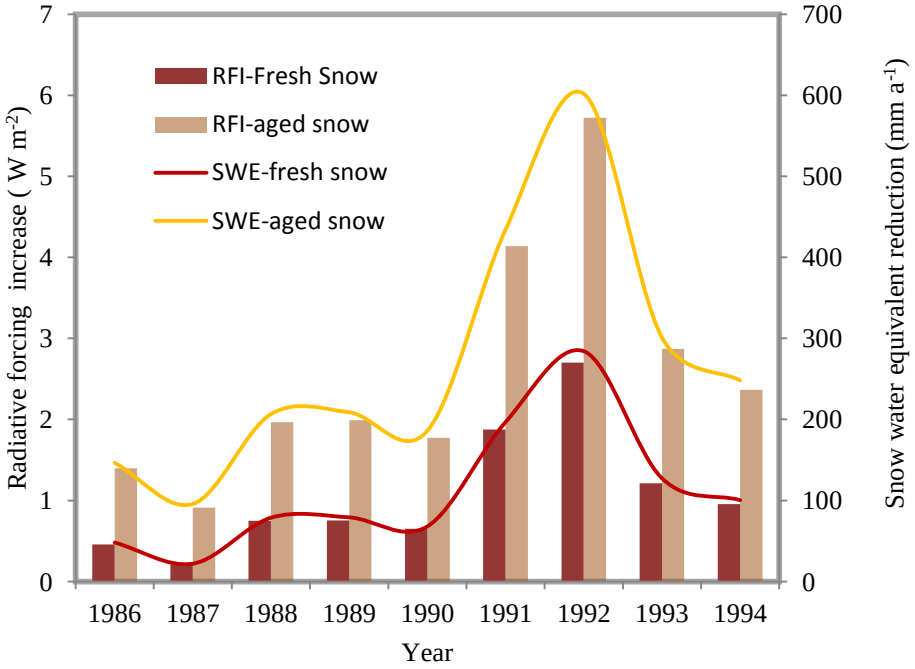

Fig 8. Estimated the effects of BC containments on annual mean radiative forcing increase (RFI) (W/m^2) and snow water equivalent (SWE) reduction (mm/a), under fresh snow assumption (purple line and bars) and aged snow assumption (yellow line and bars).

Table 1. Source regions and corresponding fractional contributions to atmospheric BC concentrations at the Muztagh Ata site in monsoon, non-monsoon and all months during 1993

	Source regions	Latitude	Longitude	Summer monsoon (June-September)	Non-monsoon (October-May)	Annual
R1	Central Asia	37-56 ℕ	50-95 ℍ	43.9%	18.1%	26.7%
R2	Europe	35-67 ℕ	0-50 ℍ	26.6%	11.5%	16.5%
R3	Persian Gulf	24-35 ℕ	35-55 ℍ	9.4%	12.1%	11.2%
R4	South Asia	14-37 ℕ	55-95 ℍ	7.3%	33.7%	24.9%
	Others	NA	NA	7.9%	6.2%	6.8%